PROCEEDINGS OF THE INTERNATIONAL CONFERENCE NANOMATERIALS: APPLICATIONS AND PROPERTIES
Vol. **1** No 4, 04MFPN18(4pp) (2012)

Synthesis and magneto-optical properties of Co nanoparticle arrays

V.A. Zlenko, M.G. Demydenko, S.I. Protsenko

Sumy State University, 2, Rymsky-Korsakov Str., 40007 Sumy, Ukraine

(Received 16 August 2012; published online 24 August 2012)

In this paper described a technique for obtaining arrays of magnetic nanoparticles on amorphous Si_3N_4 substrates during annealing of thin Co films. Magneto-optical properties of the nanoparticle arrays were studied using MOKE. It was shown the dependence of magneto-optical properties of nanoparticle arrays from their morphology.

Keywords: Magnetic nanoparticle, Coalescence, MOKE, Anisotropy.

PACS numbers: 61.46.Df, 68.37.Lp, 81.15.Ef, 75.60.Tt

1. INTRODUCTION

Much attention that scientists devote to studies of magnetic and magneto-optical properties of nanoparticles and nanostructured materials caused not only by the constant need of upgrading and improving hardware components of modern electronics [1,2]. Such systems constitute a bridge between the theories of nuclear and bulk material magnetisms.

One of the methods used in these studies is based on the magneto-optical Kerr effect (MOKE). The data obtained using MOKE can be used either for subsequent characterization and improvement of material magnetic properties or for developing a theoretical models describing and predicting this properties [3,4].

Earlier in papers [5,6] has been described technique of obtaining arrays of Cu and Ni nanoparticle arrays on amorphous polymer substrates during annealing of thin metal films in vacuum. This paper describes technique of obtaining of Co nanoparticle arrays on Si_3N_4 substrates, the change of their magneto-optical properties and morphology during thermal annealing were studied.

2. EXPERIMENTAL

To obtain ordered arrays of Co nanoparticles we used the method of the thermal dispersion of thin Co films. Thin cobalt films were obtained by thermal evaporation in vacuum system VUP-5M (residual gas pressure $P = 10^{-4}$ Pa). The effective film thicknesses were controlled using a quartz resonator method and amounted 1.5-3.5 nm. Co films were deposited on amorphous Si_3N_4 substrates. Further samples were annealed using ceramic heater Tec tra in vacuum system Pfeiffer (residual gas pressure $P = 10^{-7}$ Pa).

In order to study changes in the morphology features of Co films after their thermal annealing we used AFM (atomic force microscope Dimension Edge). Surface images were obtained in contact and tapping modes.

The use of tapping mode reduces impact force of probe on the sample surface. This mode is useful for a study of objects with very small sizes when sample surface has a small relief gradient. Image forms by recording the amplitude and phase fluctuations of cantilever. Contact mode AFM is characterized by constant mechanical interaction between probe and sample surface. This mode allows to achieve higher resolution and provides a better quality of images when scanning the surface with large relief fluctuations.

Contact mode was chosen to achieve a better resolution for samples with a more pronounced relief (effective thickness of Co 2.5 and 3.5 nm). For a sample with effective thickness of Co 1.5 nm contact mode showed worse results because of the impact of the tip of the probe to an array of nanoparticles. In this case was used tapping mode. In addition, some samples were further studied in tapping mode.

Magneto-optical properties were studied using MOKE in longitudinal measurement geometry.

3. RESULTS AND DISCUSSION

3.1 Thermal evolution of sample surface morphology

Paper [7] describes the changing of magnetic anisotropy of Fe nanoparticle arrays after annealing at different temperatures. Authors suggest a strong correlation between surface morphology and magnetic properties of the samples. It was shown that thermal annealing leads to increase in the size of nanoparticles and reorientation of magnetic anisotropy.

Examples of AFM images of as deposited Co thin films are given in Fig. 1a,b. Increase in initial effective thickness of Co leads to expected increase in the size of islands.

Studies have shown that all of Co films with an effective thickness of 1.5 (sample 1), 2.5 (sample 2) and 3.5 nm (sample 3) after deposition on Si_3N_4 substrates have island like structure. In [5,6] for obtaining ordered arrays of Cu and Ni nanoparticle arrays we used polyimide substrates, all of as deposited films had continuous structure.

The first annealing of the samples was held for 30 min at T = 1100 K. Fig. 1c,d,e gives AFM images of Co films after annealing. Results indicate the formation of cobalt nanoparticle arrays. Measurements showed that particle size distribution have unimodal character for samples 1 and 2 (nanoparticles size range 20-40 and 20-70 nm, respectively) and double modal character for sample 3 (nanoparticles size range 25-150 nm). This phenomenon is described in [8], in which investigated changes in the morphology of thin Bi and Sn thin films during the process of melting and crystallization. It was shown that increase in initial film effective thick-

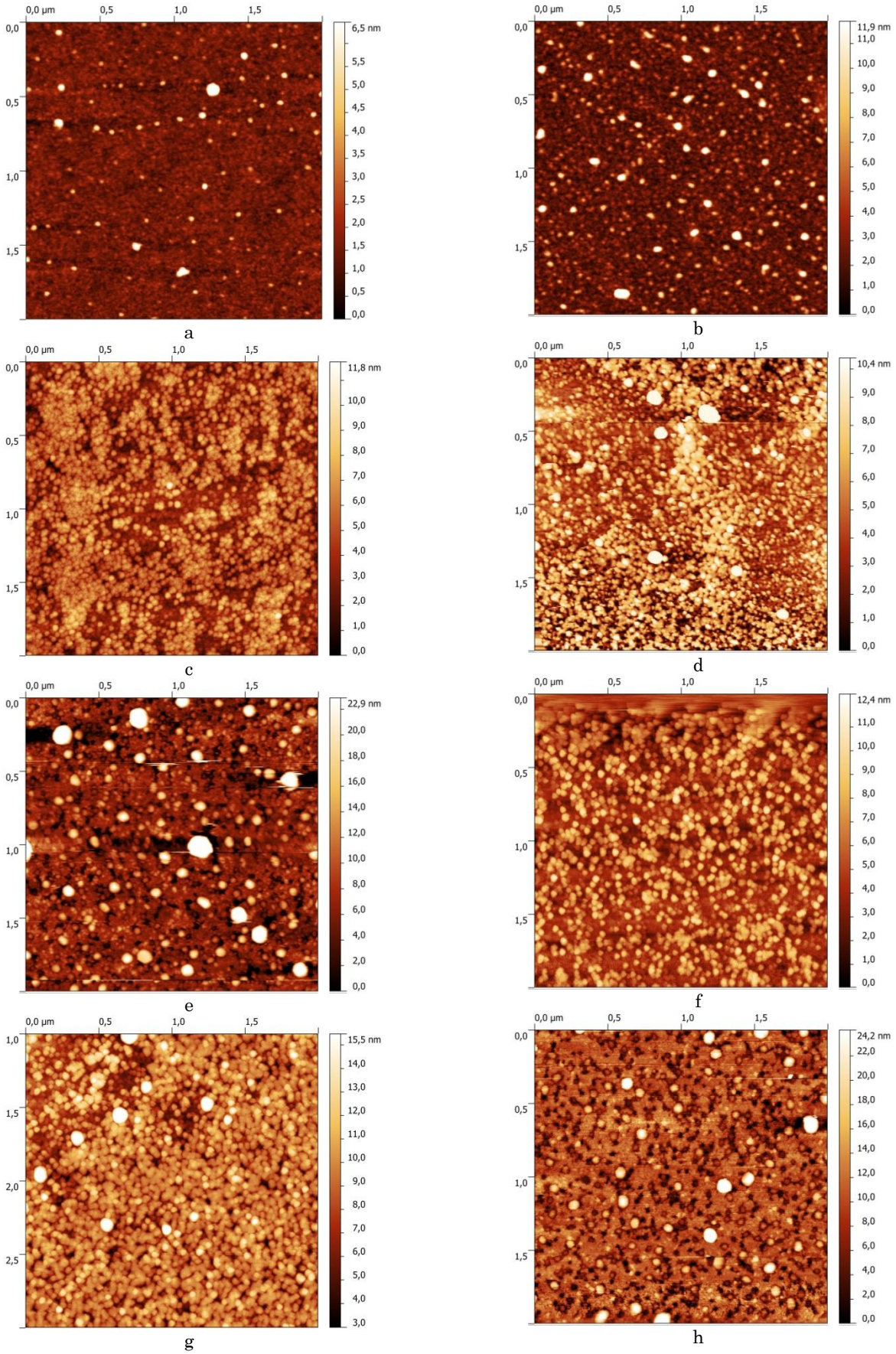

Fig. 1 – AFM images of Co films with initial effective thickness 1,5 nm (a,c,f), 2,5 nm (b,d,g), 3,5 nm (e,h) before annealing (a,b), after first (T=1100 K) (c-e) and second (T=1200 K) (f-h) annealing

ness leads to the change of particles size distribution character from unimodal to double modal.

The second annealing of samples held at T = 1200 K. AFM images of samples after second annealing are given in Fig. 1f,g,h. Obviously we observe some increase in the nanoparticles size in case of samples 1 and 2 (particles size range 25-50 and 30-80 nm, respectively). It is explained by particles coalescence. In case of sample 3 we observe some decrease in particle size (particles size range 30-110 nm), what can be explained by the transition from a flatter to a more spherical shape. It should be noted that the type of the particle size distribution after the second annealing in all three cases has not changed.

This method of Co nanoparticle synthesis was previously tested by us using polyimide substrates [5,6]. Analysis of data obtained by transmission electron microscopy showed that films with an initial effective thickness of 1.5 nm after the deposition had a structure close to continuous. Annealing of these films also led to the formation of metal nanoparticle arrays that have double modal character of the size distribution. Also it should be noted that size range of particles formed on polyimide substrates was smaller (5-20 nm) than on Si_3N_4 substrates (20-50 nm) (for initial effective thickness of Co films 1.5 nm).

3.2 Magneto-optical properties

To establish a correlation between the morphology of samples and their magneto-optical properties we made MOKE measurements before and after annealing. Study with magneto-optical Kerr effect consists in the rotation of polarization plane of linearly polarized light as it reflected from a magnetic surface, placed in a magnetic field.

The measurements for the Co films were made in longitudinal geometry at angles of 0-360°, and showed that non-annealed samples have no coercivity. Fig. 2a,c shows the dependence of MOKE signal from the quantity of magnetic field for annealed at T = 1100 K for samples 2 and 3. As can be seen thermal treatment led to appearance of hysteresis loop on the curves.

The dependence for sample with cobalt initial effective thickness 1,5 nm had a similar form, but there was practically no coercivity force. It is known that magnetic nanoparticle that has small enough size transits to the superparamagnetic state in which lose it magnetic properties. Most probably, this situation also observed in this case.
Fig. 2b,d gives MOKE data obtained after the second annealing at T = 1200 K. Graphs show that the shape of curves for samples 2 and 3 has not changed. However, it is observed some increase in coercivity and in MOKE signal order. For sample 2, this tendency most likely explained by increase in nanoparticles size due to coalescence, whereas in case of sample 3, this may be related with the change of particles shape. The appearance of hysteresis loop on MOKE dependence for the sample 1 most likely related to the overall increase in nanoparticles size during annealing However, the value of the coercivity force for this sample is much smaller than for other two. Another possible explanation may be a reorientation of the magnetization axes, associated with an increase in particles size during the thermal treatment [7, 9, 10].

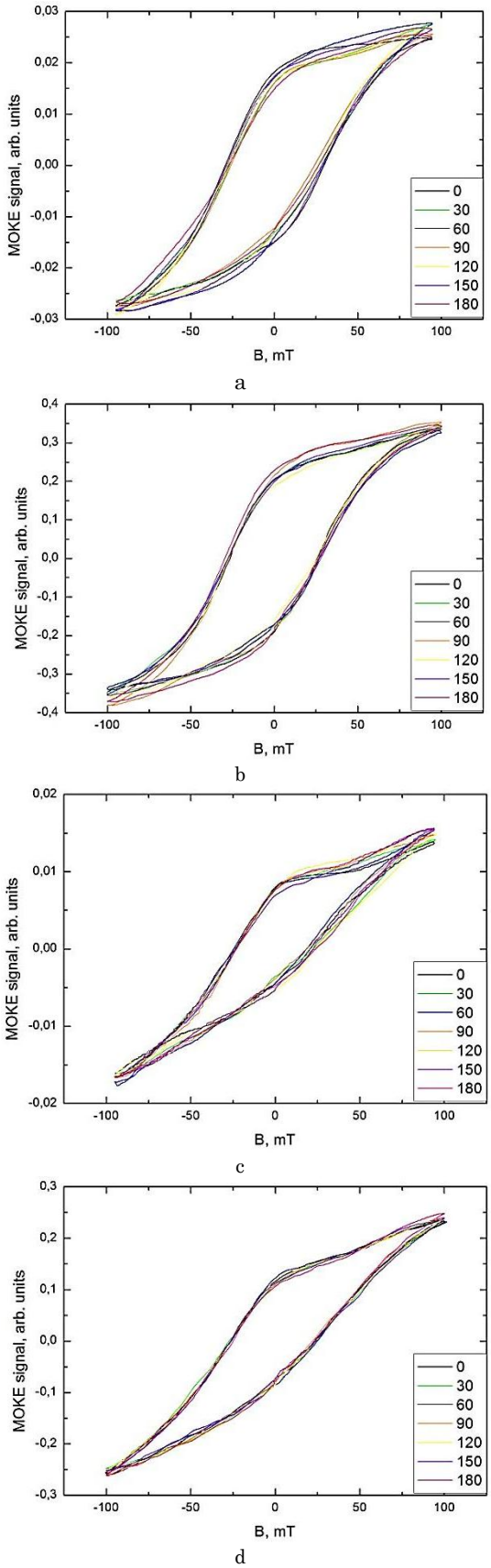

Fig. 2 – MOKE hysteresis loops, measured from sample 2 (a,b) and 3 (c,d) after first (a,c) and second (b,d) annealing . Color lines show the angle of samples rotation in the plane. The insets show the angle in degrees

Fig. 3 shows the dependences of samples coercivity from the angle of their rotation after first and second annealing. Curves show that for all samples, this value is practically independent from the angle of rotation, what can be related with absence of easy magnetization axes.

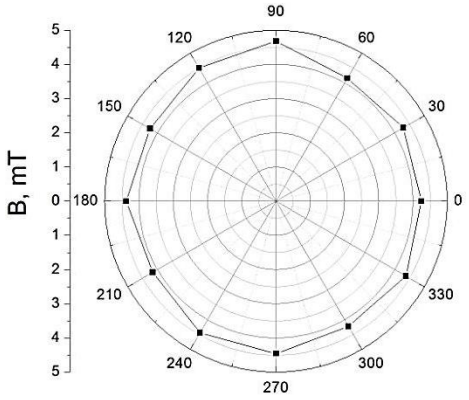

a

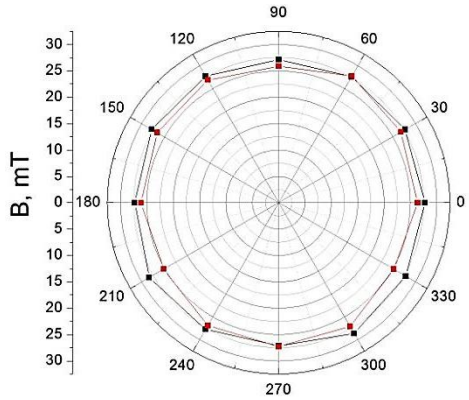

b

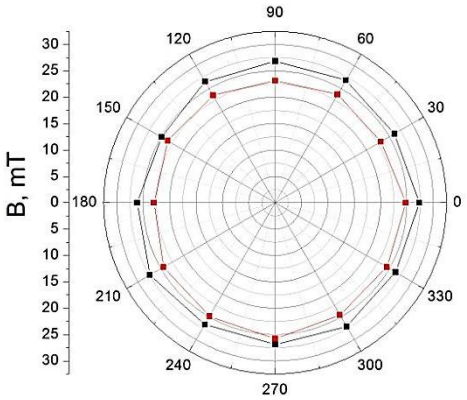

c

Fig. 3 – Dependence between angle of sample rotation and coercivity for sample 1 (a), 2(b) and 3 (c). Red lines show data, measured after first annealing, black – after second

4. CONCLUSIONS

By thermal dispersion of thin layers method obtained ordered assemblies of Co nanoparticles. The study of magnetic properties by MOKE method allows to trace the evolution of the hysteresis dependencies for nanoparticles ensemble during thermal treatment.

REFERENCES

1. D. Kumar, J. Narayan, T.K. Nath, A.K. Sharma, A. Kvit, C. Jin, *Sol. St. Commun.* **119**, 63 (2001).
2. I.V. Cheshko, S.I. Protsenko, L.V. Odnodvorets, P. Shifalovich, *Pis'ma v ZhETF* **35** No19, 53 (2009).
3. S.V. Komogortsev, S.I. Smirnov, N.A. Momot, R.S. Ishakov, *J. Sib. Fed. Univ. Math. Phys.* **3**, 515 (2010).
4. B.B. Krichevtsov, S.V. Gastev, D.S. Iluschenkov, A.V. Kaveev, N.S. Sokolov, *FTT* **51** No1, 109 (2009).
5. V.A. Zlenko, S.I. Protsenko, *Nanosystems, Nanomaterials, Nanotechnologys* **9** No3, 607 (2011).
6. V.A. Zlenko, S.I. Protsenko, *Metallofiz. Noveysh. Tehnol.* **33** No4, 495 (2011).
7. J.H. Lai, C.C. Kuo, Y.C. Liu, J.C.A. Huang, *J. Magn. Magn. Mater.* **310**, e803 (2007).
8. N.T. Gladkikh, A.P. Krishtal', R.V. Sukhov, L.N. Tchepurnaya, *VANT: Physics of radiation damage and radiation materials* **94** No4-2, 293 (2009).
9. M. Stampanoni, A. Vaterlaus, M. Aeschlimann, F. Meier, *Phys. Rev. Lett.* **59**, 2483 (1987).
10. D.S. Chuang, C.A. Ballentine, R.C. O'Handley, *Phys. Rev. B* **49**, 15084 (1994).